Local hyperthyroidism promotes pancreatic acinar cell proliferation during acute pancreatitis

Running title: Endogenous T3 supports acinar proliferation

Ermanno Malagola[1], Rong Chen[1], Marta Bombardo[1], Enrica Saponara[1] Monica Dentice[2], Domenico Salvatore[2], Theresia Reding[1], Stephen Myers[4], Andrew P. Hills[4], Rolf Graf[1,3] and Sabrina Sonda[1,3,4*]

[1]Swiss Hepato-Pancreato-Biliary Center, Department of Visceral and Transplantation Surgery, University Hospital, Zurich, Switzerland; [2]Department of Clinical Medicine and Surgery, University of Naples Federico II, Naples, Italy; [3]Center for Integrative Human Physiology (ZIHP), University of Zurich, Switzerland; [4]School of Health Sciences, College of Health and Medicine, University of Tasmania, Australia.

***Address correspondence to** Sabrina Sonda, School of Health Sciences, College of Health and Medicine, University of Tasmania, Launceston TAS 7250, Australia. Tel. +61363243248, FAX +61363243995, E-mail: sabrina.sonda@utas.edu.au

Abbreviations: 3,3',5-triiodo-L-thyronine, T3; thyroid hormone receptor beta, TRβ; TGFβ receptor II deficient mice, TGF-RII KO; deiodinase, DIO; deiodinase 3 deficient mice, D3KO; methimazole, MMI; iopanoic acid, IOP; histone deacetylases, HDAC; acinar-to-ductal metaplasia (ADM)

Disclosures: The authors have declared that no conflict of interest exists.

Word count: 3961

Abstract

Proliferation of pancreatic acinar cells is a critical process in the pathophysiology of pancreatic diseases, as limited or defective proliferation is associated with organ dysfunction and patient morbidity. In this context, elucidating the signalling pathways that trigger and sustain acinar proliferation is pivotal to develop therapeutic interventions promoting the regenerative process of the organ.

In this study we used genetic and pharmacological approaches to manipulate both local and systemic levels of thyroid hormones to elucidate their role in acinar proliferation following cerulein-mediated acute pancreatitis in mice. In addition, molecular mechanisms mediating the effects of thyroid hormones were identified by genetic and pharmacological inactivation of selected signalling pathways.

In this study we demonstrated that levels of the thyroid hormone 3,3',5-triodo-L-thyronine (T3) transiently increased in the pancreas during acute pancreatitis. Moreover, by using genetic and pharmacological approaches to manipulate both local and systemic levels of thyroid hormones, we showed that T3 was required to promote proliferation of pancreatic acinar cells, without affecting the extent of tissue damage or inflammatory infiltration.

Finally, upon genetic and pharmacological inactivation of selected signalling pathways, we demonstrated that T3 exerted its mitogenic effect on acinar cells via a tightly controlled action on different molecular effectors, including histone deacetylase, AKT, and TGFβ signaling.

In conclusion, our data suggest that local availability of T3 in the pancreas is required to promote acinar cell proliferation and provide the rationale to exploit thyroid hormone signaling to enhance pancreatic regeneration.

Keywords: thyroid hormones, T3, deiodinases, acinar proliferation, acute pancreatitis

Introduction

Acute pancreatitis, a debilitating inflammatory disease of the pancreas, is a major cause of gastrointestinal hospital admission [1]. Pancreatic injury leads to dysfunctional processes and, in severe circumstances, necrosis of exocrine pancreatic tissue, resulting in high morbidity and mortality. In this context, enhancing regeneration of the exocrine pancreas is a key therapeutic target to restore the activity of the organ and limit the pathological implications associated with impaired pancreatic function.

We aimed to identify molecular factors that act as mitogens for pancreatic acinar cells and thus have the potential to be exploited therapeutically to promote pancreatic regeneration. Fully differentiated pancreatic acinar cells are able to transiently de-differentiate to a progenitor-like state and re-enter the cell cycle program in response to pancreatitis [2]. However, this proliferative ability, reported in human and animal models, is often limited, thus hampering the extent of pancreatic regeneration. In recent years multiple signaling pathways and transcription factors have been described to be activated during acinar cell proliferation following pancreatitis (reviewed in [3]). Importantly, molecular factors involved in the process of regeneration in the adult pancreas are also implicated in the embryonic development of the organ. However, our knowledge regarding molecules that specifically trigger or sustain proliferation of acinar cells is still limited. In this study, we investigated whether a proliferative stimulus for acinar cells is provided by a local

increase of thyroid hormone levels in the pancreas upon induction of pancreatitis. The hypothesis of local hyperthyroidism to support pancreatic regeneration was built on independent lines of evidence. Firstly, consistent with the fact that a developmental program is re-activated during pancreatic regeneration, thyroid hormones play a functional role in the development of pancreatic cells during organogenesis, demonstrated in both amphibian and mammalian pancreas (reviewed in [4]). Secondly, adult acinar cells harbor the molecular machinery to respond to thyroid hormones and start proliferating when 3,3',5-triiodo-L-thyronine (T3), the biologically active thyroid hormone that binds to thyroid hormone receptors [5], is administered exogenously [6, 7]. Finally, thyroid hormones act as mitogens during regeneration of adult liver [8], an organ that shares the same embryological lineage with the pancreas.

To test our hypothesis that thyroid hormones are endogenous mitogens for pancreatic acinar cells during pancreatitis, we utilized genetic and pharmacological approaches to alter their local and systemic levels, and assessed acinar proliferation following cerulein-induced pancreatitis, the most widespread experimental method to induce the disease in rodents [3].

Materials and methods

Detailed materials and methods are described in Supplementary Information.

Animal experiments

All animal experiments were conducted in accordance with Swiss federal animal regulations and approved by the cantonal veterinary office of Zurich. All studies involving animals are reported in accordance with the ARRIVE guidelines for reporting experiments

involving animals. Pancreatitis was induced with 50 µg/kg cerulein injections in adult male C57BL/6 mice, mice with inducible ablation of Deiodinase 3 in acinar cells ($ELA^{Cre-ERT2}/D3^{flox/flox}$, D3KO) and mice with conditional ablation of TGFβ receptor II (TGF-RII KO) in the pancreas [9]. The CRE-negative littermates were used as controls.

Hyperthyroidism and hypothyroidism were induced by administration of 400 µg/kg T3 and 0.1% methimazole, respectively [10]. MS-275 and MK2206 were used to inhibit Class I histone deacetylase and AKT.

Immunohistochemistry

Histological analyses were performed on paraffin-embedded pancreas, as previously described [11].

Protein analyses

Protein expression in tissue was quantified by western blotting using pancreas homogenates in RIPA buffer. HDAC activity in pancreas was measured by ELISA assay. Enzyme activity in blood was quantified using clinical chemistry procedures.

Transcript analyses

Gene expression was quantified by qRT-PCR using Taqman probes (Applied Biosystems, Foster City, CA). Transcript levels were normalized using 18S RNA as a reference and expressed as $2^{-\Delta\Delta Ct}$ relative to the value of control animals.

Statistics

Groups of five animals were tested for each experimental group. The data are expressed as means ± SEM. The statistical significance of differences in the means of experimental groups was determined using an unpaired, two-tailed Student's *t* test or one-way analysis

of variance followed by Dunnett post-test (GraphPad Prism 7; GraphPad Software, Inc.) and a probability value <0.05 was considered statistically significant.

Results

Local hyperthyroidism is induced in the pancreas during acute pancreatitis

To test whether thyroid hormones act as mitogens during pancreatic regeneration upon inflammatory injury, we first investigated whether T3 levels increased in the pancreas following induction of acute pancreatitis with serial injections of cerulein. Cerulein administration (scheme depicted in **Fig.1A**) results in a time-dependent increase in acinar cell proliferation, as quantified by the levels of acinar cells positive for the general proliferation marker Ki67 (**Fig.1B, S1A**). Interestingly, we observed a transient surge of free T3 (F-T3) levels, the biologically active form of the hormone (reviewed in [5]), in the pancreas (**Fig.1C**), which preceded the peak of acinar cell proliferation. Conversely, levels of thyroid hormones F-T4 and F-T3 transiently decreased in blood (**Fig.1D**). Increased F-T3 levels in pancreatic tissue may derive from increased uptake from the circulation of either T3 and/or of T4, with subsequent conversion into T3 by the action of deiodinases (DIO) enzymes, which regulate the intracellular hormone concentration in a time- and tissue-specific fashion, independently on the levels present in blood [5]. We detected an early up-regulation of *Dio2*, the enzyme responsible for local T4 to T3 conversion in target cells [12], in the pancreas in response to induction of pancreatitis (**Fig.1E**). Importantly, *Dio3*, the expression of which increases upon hyperthyroid status [13-15], was also up-regulated in the pancreas. *Dio3* increase is not only an indicator of local hyperthyroidism in the pancreas, but it likely limits the hormone increase, as it is the

major inactivating enzyme terminating the action of both T4 and T3 hormones [16]. Finally, *Dio1* expression was transiently down-regulated. The mechanisms of this down-regulation are not completely elucidated, however it is possible that inflammatory cytokines released during pancreatitis contribute to reduce *Dio1* expression, as previously reported in hepatocytes [17].

Dio2 and *Dio3* up-regulation was also detected in pancreatic acinar cells isolated after 24 h of cerulein treatment (**Fig.1F**), suggesting that acinar cells are able to regulate the intracellular concentration of thyroid hormones. Analyses of *Dio* expression in multiple organs revealed that gene regulation was either detected exclusively (*Dio1, Dio2*) or showing the highest regulation (*Dio3*) in the injured pancreas (**Fig.1G**).

Collectively, these data support the hypothesis that increased levels of F-T3 and consequent local hyperthyroidism are specifically and transiently induced in the organ in response to acute pancreatitis.

Genetic ablation of DIO3 in acinar cells increases acinar proliferation during acute pancreatitis

To test whether the transient hyperthyroidism observed promotes acinar proliferation, we increased the levels of thyroid hormones in acinar cells by conditionally knocking out *Dio3* using a tamoxifen-inducible approach (scheme depicted in **Fig.2A**). In the absence of pancreatitis, *Dio3* conditional KO (D3KO) mice presented a normal phenotype indistinguishable from control mice. This was evident by normal pancreatic histology (**Fig.2B**), lack of acinar damage (**Fig.S1A**), and absence of inflammation (**Fig.2C**). Similarly, no differences in basal levels of acinar cell proliferation were observed between transgenic and control mice (**Fig.2D**), even one month after tamoxifen treatment

(**Fig.S1B**), suggesting that ablation of *Dio3* does not compromise pancreatic homeostasis in untreated mice. Similarly, levels of pancreatic and circulating thyroid hormones were not altered in D3KO mice in untreated conditions (**Fig.2E**). However, upon induction of acute pancreatitis (treatment scheme depicted in **Fig.2F**), proliferation of acinar cells was higher in D3KO animals, as determined by the number of Ki67 positive cells (**Fig. 2G**) and cyclin expression in the pancreas (**Fig.2H**). Consistent with Dio3 ablation, D3KO animals showed increased levels of F-T3 in the pancreas (**Fig.2I**). The limited extent of T3 increase is likely the result of the relatively low recombination efficiency reported for this line [18, 19]. Increased acinar proliferation was not a consequence of increased pancreatic injury upon induction of pancreatitis, as blood levels of amylase and lipase, the most reliable indicators of acinar cell damage, were comparable in control and D3KO mice (**Fig.2J**). Similarly, increased proliferation was not driven by increased recruitment of PU.1-positive inflammatory cells, as their number was comparable in the two strains (**Fig.2K**). Finally, increased acinar proliferation was not accompanied by changes in the levels of acinar-to-ductal metaplasia (ADM) (**Fig.2L**), a transient de-differentiation of acinar cells observed in the tissue during pancreatic regeneration. Collectively, these data indicate that ablation of *Dio3* in acinar cells is sufficient to increase pancreatic levels of F-T3 and to enhance acinar proliferation upon induction of acute pancreatitis.

Systemic alterations of thyroid hormone levels modulate acinar cell proliferation during acute pancreatitis

After showing that local hyperthyroidism supports acinar proliferation, we then investigated whether systemic alteration of thyroid hormone levels affect the extent of

acinar proliferation during the disease. Systemic hyperthyroidism was induced by daily administration of T3 starting after the first set of cerulein injections, while systemic hypothyroidism was induced by administration of $NaClO_4$ and methimazole (MMI) for 28 days (regimen scheme depicted in **Fig.3A**). Analysis of thyroid hormone levels in serum confirmed the efficacy of the treatments as T3 administration increased F-T3 levels and decreased F-T4, as a consequence of negative feedback loop, while MMI administration decreased the levels of both hormones (**Fig.3B**).

T3 treatment significantly increased proliferation of acinar cells (**Fig.3C, S2A**), and cyclin expression in the pancreas (**Fig.3D**). Conversely, MMI administration decreased both acinar proliferation and cyclin expression (**Fig.3C, D**). In addition, thyroid hormone alterations did not affect the average size of acinar cells (**Fig. S2B**), suggesting that this parameter is not correlated with the level of cell proliferation.

Administration of T3 to hypothyroid mice rescued the defective acinar proliferation (**Fig.3E**), further demonstrating that increased levels of this hormone are sufficient to boost acinar cell proliferation.

The observed changes in acinar proliferation were not a consequence of changes in initial damage of acinar cells or infiltration of inflammatory cells, as shown by comparable levels of serum amylase and lipase (**Fig.3F**). Levels of lactate dehydrogenase (LDH), an additional marker of tissue damage, were also comparable 8 hours after induction of pancreatitis (**Fig. S3**). Furthermore, differences in acinar replication were not correlated to differences in infiltration of PU.1-positive inflammatory cells (**Fig.3G**), acinar apoptosis (**Fig.S4A**) or DNA damage (**Fig.S4B**). Collectively, these data suggest that altering the systemic levels of thyroid hormones does not modify pancreatic sensitivity to cerulein

administration and recruitment of inflammatory cells. In addition, changes in acinar proliferation induced by systemic variation of thyroid hormone levels are independent from the levels of acinar cell injury and inflammatory cell infiltration.

Finally, to demonstrate that T3 sustains acinar cell proliferation independently from T4, we administered Iopanoic acid (IOP), a specific deiodinase inhibitor that blocks T4 to T3 conversion [20], in combination with cerulein (**Fig.3H**). Analysis of thyroid hormone levels confirmed that IOP administration decreased blood levels of F-T3, whereas F-T4 amount was unchanged (**Fig.3I**). Similar to what we observed in hypothyroid mice, IOP-treated animals showed a significant decrease in the number of proliferating acinar cells (**Fig.3J**). Overall, these data demonstrate the existence of a positive correlation between thyroid hormone levels, in particular T3 availability, and proliferation of acinar cells in response to acute pancreatitis.

Acinar proliferation induced by T3 administration is promoted by HDAC activity and AKT signaling

Next, we investigated the molecular mechanisms underlying the mitogenic action of T3 in pancreatic acinar cells. To focus exclusively on T3 action without the confounding aspect of pancreatic inflammation, we supplemented T3 *in vivo* in the absence of cerulein-induced pancreatitis (scheme depicted in **Fig.4A**). Analysis of acinar cells positive for proliferation markers Ki67 and pH3 (**Fig.4B**) and pancreatic expression of early and late cyclins (**Fig.S5A**) showed that T3 exerted a profound mitogenic effect on acinar cells 96 hours after the beginning of the treatment, as previously described [6]. Moreover, T3-mediated induction of acinar proliferation was dose-dependent (**Fig.4C**) and it did not elicit inflammatory cell infiltration (**Fig.4D**) or morphological alteration of pancreatic tissue

(**Fig.S5B**), which further support our observation that T3 does not influence pancreatic inflammation during the development of pancreatitis. As previously reported, systemic administration of T3 results in proliferation of different cell types, including cardiomyocytes [21-23] (**Fig.S6A**). However, T3 did not stimulate the replication of pancreatic islet cells in our experimental conditions (**Fig. S6B**).

T3 regulates multiple pathways within the cells by genomic and non-genomic actions [24]. Here we tested whether T3 activates signaling pathways that are known to support acinar proliferation during pancreatitis. We first assessed whether T3 administration triggered the upregulation of histone deacetylases (HDAC), a class of epigenetic modifiers activated during pancreatitis and promoting proliferation of acinar cells [25, 26]. T3 treatment was sufficient to increase both the expression of different HDAC isoforms (**Fig.4E**) and total HDAC activity in the pancreas (**Fig.4F**). *In vivo* treatment with the specific class I HDAC inhibitor MS-275 (treatment scheme depicted in **Fig.S7A**) effectively reduced HDAC activation (**Fig.S7B**) and reduced acinar cell proliferation (**Fig.4G**), suggesting that increased HDAC activity is required for the mitogenic effect mediated by T3. At the molecular level, inhibition of acinar cell proliferation was accompanied by reduced cyclin B expression (**Fig.S7C**) and increased expression of cell cycle inhibitors, including p15 (Cdkn2b), p16 (Cdkn2a), and p18 (Cdkn2c) (**Fig.S7D**).

We then investigated whether T3 administration promoted the activation of phosphatidylinositol 3-kinase (PI3K)/AKT signaling. The AKT pathway is important for pancreatic proliferation, as reduction of this signaling suppresses acinar cell division [27] and its constitutive activation in adult acinar cells leads to excessive proliferation and malignant transformation [28]. T3 supplementation significantly increased pancreatic

gene expression of *Akt1* and *Akt2* isoforms (**Fig.4H**), AKT protein levels and AKT activation via phosphorylation (**Fig.4I**). To test the functional relevance of AKT signaling, we administered the potent pan-AKT inhibitor MK-2206, effective *in vivo* [29]. MK-2206-treated mice (treatment scheme depicted in **Fig.S8A**) showed reduced AKT activation (**Fig.4J**), confirming the efficacy of the compound. Importantly, MK-2206 treatment strongly reduced acinar cell proliferation (**Fig.4K**) and cyclin expression (**Fig.S8B**) while increasing the expression of the cell cycle inhibitors *p15* (Cdkn2b), and *p16* (Cdkn2a), (**Fig.S8C**), which could likely contribute to the observed inhibition of proliferation.

Collectively, these data demonstrate that T3 promotes the proliferation of healthy acinar cells by activating signaling pathways known to support acinar proliferation during pancreatitis.

Acinar proliferation induced by T3 administration is restrained by TGFβ signaling.

We then investigated whether pathways inhibiting cell proliferation are also engaged upon T3 administration. This is an important component in organ regeneration as activation of pro- and anti-mitogenic signaling is also observed during pancreatitis, thus resulting in a tightly controlled acinar cell proliferation. Transforming Growth Factor beta (TGFβ) signaling via TGFβ receptor II is activated in pancreatic cells during cerulein-induced pancreatitis and it reduces acinar cell proliferation [9]. Expression levels of TGFβ1–*3* isoforms increased in the pancreas at 96 hours following T3 supplementation (**Fig.5A**). However, increased expression of TGFβ isoforms was not accompanied by a robust increase in phosphorylation of SMAD effector proteins at this time point (**Fig.5B**), suggesting that activation of TGFβ signaling is blunted in the presence of T3.

To investigate whether the observed upregulation of TGFβ exerts an anti-mitogenic action, we assessed the levels of T3-induced acinar cell proliferation in mice lacking TGFβ signaling following ablation of TGFβ receptor II in the pancreas, which we characterized previously in the context of pancreatitis [9] (scheme depicted in **Fig.5C**). Similar to what we observed upon cerulein administration and inflammatory injury, acinar proliferation induced by T3 treatment increased in the absence of TGFβ receptor II, as quantified by the levels of proliferation markers (**Fig.5D**) and cyclin expression (**Fig.S9A**). T3 treatment did not change robustly the expression of cell cycle inhibitors (**Fig.S9B**). Overall, our data suggest that acinar cell proliferation induced upon T3 administration is restrained by TGFβ signaling.

Discussion

Thyroid hormones play essential roles in the embryonic and adult homeostasis across species, by regulating the development of several organs, growth and metabolic processes [12].

Here we showed that thyroid hormone signaling is activated during the pathological setting of pancreatitis where it promotes pancreatic acinar cell proliferation.

These findings have important implications for translational application in a therapeutic setting, as defective or limited acinar proliferation is at the core of morbidity associated not only with acute pancreatitis but also with acinar atrophy and exocrine pancreatic insufficiency found in a broader range of pancreatic diseases, including chronic pancreatitis, diabetes and cystic fibrosis.

Our results highlight three major concepts that demonstrate the profound effect exerted by thyroid hormones in the pathophysiology of pancreatitis. Firstly, we showed that levels of F-T3, the biologically active form of thyroid hormones, transiently increased in the pancreas following inflammatory injury. This local hyperthyroidism was determined by direct quantification of the hormone in the tissue, by organ-specific up-regulation of enzymes responsible for thyroid hormone synthesis (reported also in a recently transcriptome-based study [30]) and by up-regulation of thyroid hormone inactivating enzyme deiodinase 3, an accurate functional marker of thyroid hormone status [31, 32].

The increase of F-T3 levels in the injured pancreas was independent from circulating levels of thyroid hormones, which decreased in the initial stages of the disease. This suggests that serum hormone levels are not a direct measure of the intracellular T3 availability in the organ. In addition, the transient nature of T3 increase in the organ implies that the concentration and consequent signaling of the hormone is controlled by the activity of both activating and inactivating deiodinases engaged in a time-dependent manner in the tissue, as further supported by our deiodinases expression data.

Secondly, we revealed that selectively increasing F-T3 levels in the pancreas, by reducing deiodinase 3-dependent T3 inactivation, boosted acinar proliferation in the context of pancreatic injury. This mitogenic effect was exquisitely acinar-specific, as it did not affect replication of non-acinar cells and was not accompanied by changes in tissue damage, infiltration of inflammatory cells, or trans-differentiation of acinar cells into ADM. In addition, we showed that deiodinase 3 ablation in untreated conditions did not increase T3 levels in the pancreas nor induced proliferation of acinar cells, suggesting that an initial

pancreatic damage is necessary to trigger local hyperthyroidism and its consequent mitogenic effects.

Thirdly, we demonstrated that manipulating the circulating levels of thyroid hormones had a direct impact on acinar cell proliferation. This raises the important clinical implication that hypothyroid patients may suffer from impaired acinar proliferation in the context of pancreatitis. This potential concern complements previous reports showing that low thyroid hormone levels in acute pancreatitis patients are a marker for increased severity of the disease [33, 34].

Collectively, our data showing enhanced acinar proliferation induced by both tissue specific and systemic elevation of thyroid hormones provide a proof of concept for a potential therapeutic target to improve organ regeneration. While systemic T3 administration did not provoke adverse outcomes of tissue damage or inflammation (our study and [6, 7]), T3 exerts mitogenic effects in different organs. Thus, future research should focus on the development of therapeutic interventions promoting proliferation of acinar cells in a selective manner during the regenerative phase of the organ. In this context, our data suggest that inhibition of deiodinase 3 activity is an appealing target to increase T3 levels locally in the pancreas, as its expression was greatly up-regulated in the injured organ and its ablation was sufficient to increase acinar proliferation.

An additional focus of our study was to identify molecular pathways activated during T3-induced acinar proliferation. By using the controlled setting of T3 administration in the absence of pancreatitis, we demonstrated that T3 triggers the production of several signaling molecules, the activity of which either promotes or reduces acinar proliferation. This array of regulatory mechanisms provides the underlining explanation for the fact that

T3-induced acinar proliferation is a temporally controlled process. Importantly, they revealed that the signaling pathways activated by T3 are also crucial in regulating acinar proliferation in the context of pancreatitis [9, 26, 27], further supporting the concept that T3 is a major factor in driving acinar cell division upon inflammatory insult.

Amongst the pathways identified, we discovered that T3-induced acinar proliferation is promoted by the activity of the epigenetic modifier class I HDACs and by AKT signaling. HDACs are known members of the thyroid receptor co-repressor complex regulating the genomic effects of T3-induced transcription [35], while AKT signaling is considered an example of non-genomic actions of thyroid hormones, which are rapid in their onset and independent from nuclear uptake of T3 (reviewed in [24, 36]). Thus, the dual activation of genomic and non-genomic pathways suggests that both modality of T3 signaling are engaged in the pancreas to drive acinar proliferation. This is consistent with AKT contributing to mediate the effects of T3 administration reported in other tissues and cells, including skeletal muscle [37], heart [38] and fibroblasts [39], suggesting that activation of non-genomic actions is a common pathway in T3-mediated signaling.

The third signaling pathways we identified in the pancreas in response to T3 administration is TGFβ. Interestingly, while TGFβ isoforms were upregulated during T3 treatment, activation of TGFβ signaling was blunted. This in agreement with a previous report showing that T3 antagonizes TGFβ signaling by reducing SMAD phosphorylation [40]. The functional relevance of this signaling inhibition is likely to promote acinar proliferation, as defective TGFβ receptor potentiated the mitogenic effect of T3 in acinar cells. In this context, it is tempting to speculate the existence of a negative feedback loop where TGFβ is upregulated as a consequence of T3-driven proliferation and it acts as a

repressor of cell division. Interestingly, the cross-talk between T3 and TGFβ is not always of antagonistic nature. As an example, T3 administration activates TGFβ signaling in hepatocellular carcinoma and results in reduced cell proliferation [41].

Conclusions

Based on our collective results, we propose that establishment of a time-dependent and tightly controlled local hyperthyroidism in the pancreas supports acinar proliferation following injury. This discovery harbors therapeutic implications and highlights the potential of interventional strategies based on the modulation of thyroid hormonal signal to promote pancreatic regeneration.

The mitogenic effect exerted by T3 in adult pancreatic acinar cells is shared by several tissues and cell types, including renal proximal tubular epithelial cells [7], heart cells [42], liver cells [43-45]. However, a different situation is observed during muscle regeneration, where T3 is required to differentiate the local population of satellite stem cells into mature muscle cells [46]. Similarly, low levels of thyroid hormones maintain the renewal capacity of oligodendrocyte progenitor cells, while their elevation promotes the switch from stem cell proliferation to cell differentiation [47]. Intriguingly, but not entirely surprising given the pivotal role of cancer stem cells to self-renew and drive tumorigenesis [48], low levels of thyroid hormones are required to support the development of different malignancies (reviewed in [49]).

Thus, our results contribute to expand the concept that thyroid hormones induce different outcomes in different replicative contexts where they control the balance between proliferation and differentiation. While this study provides the first insight into endocrine regulation of acinar proliferation, further studies are required to elucidate fully the details

of thyroid hormone actions in the pancreas. An open question not addressed in our study is the identification of the thyroid hormone receptors involved in the observed phenotype and the characterization of their cistromes *in vivo*. This is of special interest as the receptor isoforms have different repertoires of target genes [50], the expression of which can be affected by thyroid hormone binding in either a positive or negative manner [51].

Another open question concerns the role of transmembrane transporters for thyroid hormones [52, 53] in regulating hormone availability in the pancreas. While a thorough characterization of transporter families has not been performed in acinar cells, it is worth mentioning that amongst the L-type amino acid transporters involved in thyroid hormone uptake, Lat1 and Lat2 are expressed on the basolateral membrane of adult acinar cells [54].

Finally, the investigation of the upstream signals that regulate expression of deiodinases in the injured pancreas is of major interest. Their identification is crucial not only to understand how the onset of local hyperthyroidism takes place, but also to identify possible targets to exploit as therapeutic intervention.

Acknowledgments

The authors thank Udo Ungethuem, Ursula Suess and Monica Seiler for excellent technical assistance. This research received grants from the Swiss National Science Foundation (Grant No. 310030–146725) and the Amélie Waring Foundation.

Author contributions: The authors of this manuscript contributed in the study design, acquisition, analysis, interpretation of data, and critical revision of the manuscript. EM

performed experiments, generated and analyzed data, drafted the manuscript; RC, MB, ES, TR performed experiments, generated and analyzed data; MD, DS, SM, APH, RG revised the manuscript; SS designed the study, wrote the manuscript. All authors approved the submitted version.

SUPPLEMENTARY INFORMATION

Detailed Materials and Methods and 7 supplementary figures are available as supplementary information.

Figure legends

Figure 1. Pancreatic levels of F-T3 increase following cerulein-induced pancreatitis. **(A)** Schematic representation of cerulein (Cer) administration. Mice received six injections daily over two consecutive days. Harvest time is indicated as hours after the first cerulein injection. **(B)** Quantification of acinar cells positive for the replication marker Ki67 at the indicated time after cerulein administration. Right panels, representative microphotograph of stained cells (partial field of view). A complete field of view of a microphotograph used for cell counting is shown in Fig. S1A. **(C)** Quantification of free T3 (F-T3) in the pancreas at the indicated time after cerulein administration. **(D)** Quantification of free T4 and free T3 in the mice sera at the indicated time after cerulein administration. **(E)** qPCR of deiodinase (DIO) 1-3 in the pancreas at the indicated time after cerulein administration. **(F)** qPCR of deiodinase (DIO) 1-3 in pancreatic acini isolated 24 hours after cerulein administration. Right panel, representative microphotographs of isolated acini. **(G)** qPCR

of deiodinase (DIO) 1-3 in different organs at the indicated time after cerulein administration. Results are average ± SEM (n=5), *P < 0.05. Scale bars: 50 μm.

Figure 2. Ablation of deiodinase 3 in acinar cells increases acinar proliferation following induction of pancreatitis. (A) Schematic representation of conditional deiodinase 3 knocked out breeding. **(B)** Hematoxylin and Eosin (H&E) staining of pancreata in wild type (WT) and deiodinase 3 knocked out (D3KO) mice in untreated conditions (partial field of view). **(C)** Quantification of PU.1-positive inflammatory cells in untreated WT and D3KO mice. Right panels, representative microphotographs of stained cells (arrows) (partial field of view). **(D)** Quantification of Ki67-positive acinar and interstitial cells in untreated mice. Right panels, representative microphotographs of stained acinar (arrows) and interstitial (arrowheads) cells (partial field of view). **(E)** Quantification of pancreatic and serum levels of free T3 (F-T3) and free T4 (F-T4) in untreated mice. **(F)** Schematic representation of induction of pancreatitis with cerulein injections in WT and D3KO mice. **(G)** Quantification of Ki67-positive acinar cells at the indicated time following induction of pancreatitis. Right panels, representative microphotographs of stained cells 96h after pancreatitis induction (partial field of view). **(H)** qPCR of cyclin expression in the pancreas at the indicated time following induction of pancreatitis. Cyclin A (*Ccna1*), cyclin B (*Ccnb1*), cyclin D (*Ccnd1*), cyclin E (*Ccne1*). **(I)** Quantification of free T3 in the pancreas at the indicated time following induction of pancreatitis. **(J)** Quantification of amylase and lipase activity in serum at the indicated time following induction of pancreatitis. **(K)** Quantification of PU.1-positive inflammatory cells at the indicated time after induction of pancreatitis. Right panels, representative microphotographs of stained cells (arrows) (partial field of view). **(L)** Quantification of

ADM 96 hours after induction of pancreatitis. Right panel, representative microphotograph of ADM area (asterisk) (partial field of view). Results are average ± SEM (n=5), *P < 0.05. Scale bars: 50 μm.

Figure 3. Systemic alteration of thyroid hormone levels affects acinar proliferation following induction of pancreatitis. (A) Schematic representation of pancreatitis induction upon hyperthyroidism (i) and hypothyroidism (II) with T3 and MMI administration, respectively. **(B)** Quantification of serum levels of free T4 (F-T4) and free T3 (F-T3) 96 hours after induction of pancreatitis. **(C)** Quantification of Ki67 and pH3-positive acinar cells 72 and 96 hours after induction of pancreatitis. Left panels, representative microphotographs of stained cells 96 hours after pancreatitis induction (partial field of view). **(D)** qPCR of cyclin expression in the pancreas at the indicated time following induction of pancreatitis. Cyclin A (*Ccna1*), cyclin B (*Ccnb1*), cyclin D (*Ccnd1*), cyclin E (*Ccne1*). **(E)** Quantification of Ki67-positive acinar cells 96 hours after induction of pancreatitis. **(F)** Quantification of amylase and lipase activity in serum at the indicated time following induction of pancreatitis. **(G)** Quantification of PU.1-positive inflammatory cells at the indicated time after induction of pancreatitis. **(H)** Schematic representation of pancreatitis induction upon IOP treatment. **(I)** Quantification of serum levels of free T4 (F-T4) and free T3 (F-T3) at the indicated time after induction of pancreatitis. **(J)** Quantification of Ki67 and pH3-positive acinar cells at the indicated time after induction of pancreatitis. Right panels, representative microphotographs of stained cells 96 hours after induction of pancreatitis (partial field of view). Results are average ± SEM (n=5), *P < 0.05. Scale bars: 50 μm.

Figure 4. T3-induced acinar proliferation is supported by HDAC activity and AKT signaling. (A) Schematic representation of T3 treatment. **(B)** Quantification of Ki67 and pH3-positive acinar cells 96 hours after 400 μg/kg T3 treatment. **(C)** Quantification of Ki67-positive acinar cells 96 hours after T3 treatment at the indicated concentrations. **(D)** Quantification of PU.1-positive inflammatory infiltrating the pancreas 96 hours after T3 treatment. **(E)** qPCR of class I and class II HDAC expression in the pancreas 96 hours after T3 treatment. **(F)** Quantification of HDAC activity in the pancreas 96 hours after T3 treatment. **(G)** Quantification of Ki67 and pH3-positive acinar cells 96 hours after T3 treatment in the presence of the selective class I HDAC inhibitor MS-275 (MS). Right panels, representative microphotographs of stained cells (partial field of view). **(H)** qPCR of AKT isoform expression in the pancreas 96 hours after T3 treatment. **(I)** Western blot analyses of AKT expression and activation in the pancreas 96 hours after T3 treatment. **(J)** Western blot analyses of AKT activation in the pancreas 96 hours after T3 treatment in the presence of the selective AKT inhibitor MK-2206 (MK). **(K)** Quantification of Ki67 and pH3-positive acinar cells 96 hours after T3 treatment in the presence of the selective AKT inhibitor MK-2206 (MK). Right panels, representative microphotographs of stained cells (partial field of view). Results are average ± SEM (n=5), *P < 0.05. Scale bars: 50 μm.

Figure 5. T3-induced acinar proliferation is restrained by TGFβ signaling. (A) qPCR of TGFβ isoform expression in the pancreas 96 hours after T3 treatment. **(B)** Western blot analyses of SMAD expression and activation in the pancreas 96 hours after T3 treatment. **(C)** Schematic representation of T3 treatment in wild type (WT) and TGFβ receptor II knocked out mice (KO). **(D)** Quantification of Ki67 and pH3-positive acinar cells

96 hours after T3 treatment in WT and KO mice. Right panels, representative microphotographs of stained cells (partial field of view). Results are average ± SEM (n=5), *P < 0.05. Scale bars: 50 μm.

References

1. Peery AF, Dellon ES, Lund J, et al. Burden of gastrointestinal disease in the United States: 2012 update. *Gastroenterology*. 2012;**143**(5):1179-87 e1-3.
2. Jensen JN, Cameron E, Garay MV, et al. Recapitulation of elements of embryonic development in adult mouse pancreatic regeneration. *Gastroenterology*. 2005;**128**(3):728-41.
3. Murtaugh LC, Keefe MD. Regeneration and repair of the exocrine pancreas. *Annu Rev Physiol*. 2015;**77**:229-49.
4. Mastracci TL, Evans-Molina C. Pancreatic and Islet Development and Function: The Role of Thyroid Hormone. *J Endocrinol Diabetes Obes*. 2014;**2**(3).
5. Abdalla SM, Bianco AC. Defending plasma T3 is a biological priority. *Clin Endocrinol (Oxf)*. 2014;**81**(5):633-41.
6. Ledda-Columbano GM, Perra A, Pibiri M, et al. Induction of pancreatic acinar cell proliferation by thyroid hormone. *J Endocrinol*. 2005;**185**(3):393-9.
7. Ohmura T, Katyal SL, Locker J, et al. Induction of cellular DNA synthesis in the pancreas and kidneys of rats by peroxisome proliferators, 9-cis retinoic acid, and 3,3',5-triiodo-L-thyronine. *Cancer Res*. 1997;**57**(5):795-8.
8. Cervinkova Z, Simek J. Effect of propylthiouracil on liver regeneration in rats after partial hepatectomy. *Physiol Res*. 1992;**41**(2):141-6.
9. Grabliauskaite K, Saponara E, Reding T, et al. Inactivation of TGFbeta receptor II signalling in pancreatic epithelial cells promotes acinar cell proliferation, acinar-to-ductal metaplasia and fibrosis during pancreatitis. *J Pathol*. 2016;**238**(3):434-45.
10. Zavacki AM, Ying H, Christoffolete MA, et al. Type 1 iodothyronine deiodinase is a sensitive marker of peripheral thyroid status in the mouse. *Endocrinology*. 2005;**146**(3):1568-75.
11. Silva A, Weber A, Bain M, et al. COX-2 is not required for the development of murine chronic pancreatitis. *Am J Physiol Gastrointest Liver Physiol*. 2011;**300**(6):G968-75.
12. Kress E, Samarut J, Plateroti M. Thyroid hormones and the control of cell proliferation or cell differentiation: paradox or duality? *Mol Cell Endocrinol*. 2009;**313**(1-2):36-49.

13. Escobar-Morreale HF, Obregon MJ, Hernandez A, et al. Regulation of iodothyronine deiodinase activity as studied in thyroidectomized rats infused with thyroxine or triiodothyronine. *Endocrinology*. 1997;**138**(6):2559-68.
14. Tu HM, Legradi G, Bartha T, et al. Regional expression of the type 3 iodothyronine deiodinase messenger ribonucleic acid in the rat central nervous system and its regulation by thyroid hormone. *Endocrinology*. 1999;**140**(2):784-90.
15. Barca-Mayo O, Liao XH, Alonso M, et al. Thyroid hormone receptor alpha and regulation of type 3 deiodinase. *Mol Endocrinol*. 2011;**25**(4):575-83.
16. Huang SA, Bianco AC. Reawakened interest in type III iodothyronine deiodinase in critical illness and injury. *Nat Clin Pract Endocrinol Metab*. 2008;**4**(3):148-55.
17. Yu J, Koenig RJ. Regulation of hepatocyte thyroxine 5'-deiodinase by T3 and nuclear receptor coactivators as a model of the sick euthyroid syndrome. *J Biol Chem*. 2000;**275**(49):38296-301.
18. Means AL, Meszoely IM, Suzuki K, et al. Pancreatic epithelial plasticity mediated by acinar cell transdifferentiation and generation of nestin-positive intermediates. *Development*. 2005;**132**(16):3767-76.
19. Desai BM, Oliver-Krasinski J, De Leon DD, et al. Preexisting pancreatic acinar cells contribute to acinar cell, but not islet beta cell, regeneration. *J Clin Invest*. 2007;**117**(4):971-7.
20. Safer JD, Persons K, Holick MF. A thyroid hormone deiodinase inhibitor can decrease cutaneous cell proliferation in vitro. *Thyroid*. 2009;**19**(2):181-5.
21. Wadosky KM, Berthiaume JM, Tang W, et al. MuRF1 mono-ubiquitinates TRalpha to inhibit T3-induced cardiac hypertrophy in vivo. *J Mol Endocrinol*. 2016;**56**(3):273-90.
22. do Imperio GE, Ramos IP, Santiago LA, et al. The Impact of a Non-Functional Thyroid Receptor Beta upon Triiodotironine-Induced Cardiac Hypertrophy in Mice. *Cell Physiol Biochem*. 2015;**37**(2):477-90.
23. Ledda-Columbano GM, Molotzu F, Pibiri M, et al. Thyroid hormone induces cyclin D1 nuclear translocation and DNA synthesis in adult rat cardiomyocytes. *FASEB J*. 2006;**20**(1):87-94.
24. Davis PJ, Davis FB, Cody V. Membrane receptors mediating thyroid hormone action. *Trends Endocrinol Metab*. 2005;**16**(9):429-35.
25. Eisses JF, Criscimanna A, Dionise ZR, et al. Valproic Acid Limits Pancreatic Recovery after Pancreatitis by Inhibiting Histone Deacetylases and Preventing Acinar Redifferentiation Programs. *Am J Pathol*. 2015;**185**(12):3304-15.
26. Bombardo M, Saponara E, Malagola E, et al. Class I histone deacetylase inhibition improves pancreatitis outcome by limiting leukocyte recruitment and acinar-to-ductal metaplasia. *Br J Pharmacol*. 2017;**174**(21):3865-80.
27. Takahashi H, Okamura D, Starr ME, et al. Age-dependent reduction of the PI3K regulatory subunit p85alpha suppresses pancreatic acinar cell proliferation. *Aging Cell*. 2012;**11**(2):305-14.
28. Elghazi L, Weiss AJ, Barker DJ, et al. Regulation of pancreas plasticity and malignant transformation by Akt signaling. *Gastroenterology*. 2009;**136**(3):1091-103.
29. Hu C, Dadon T, Chenna V, et al. Combined Inhibition of Cyclin-Dependent Kinases (Dinaciclib) and AKT (MK-2206) Blocks Pancreatic Tumor Growth and Metastases in Patient-Derived Xenograft Models. *Mol Cancer Ther*. 2015;**14**(7):1532-9.
30. Boggs K, Wang T, Orabi AI, et al. Pancreatic gene expression during recovery after pancreatitis reveals unique transcriptome profiles. *Sci Rep*. 2018;**8**(1):1406.

31. Hernandez A. Structure and function of the type 3 deiodinase gene. *Thyroid*. 2005;**15**(8):865-74.
32. Huang SA. Physiology and pathophysiology of type 3 deiodinase in humans. *Thyroid*. 2005;**15**(8):875-81.
33. Yang N, Zhang DL, Hao JY, et al. Serum levels of thyroid hormones and thyroid stimulating hormone in patients with biliogenic and hyperlipidaemic acute pancreatitis: Difference and value in predicting disease severity. *J Int Med Res*. 2016;**44**(2):267-77.
34. De Sola C, Redondo M, Pallares F, et al. Thyroid function in acute pancreatitis. *Rev Esp Enferm Dig*. 1998;**90**(1):15-22.
35. Brent GA. Mechanisms of thyroid hormone action. *J Clin Invest*. 2012;**122**(9):3035-43.
36. Davis PJ, Goglia F, Leonard JL. Nongenomic actions of thyroid hormone. *Nat Rev Endocrinol*. 2016;**12**(2):111-21.
37. Salvatore D, Simonides WS, Dentice M, et al. Thyroid hormones and skeletal muscle--new insights and potential implications. *Nat Rev Endocrinol*. 2014;**10**(4):206-14.
38. Suarez J, Scott BT, Suarez-Ramirez JA, et al. Thyroid hormone inhibits ERK phosphorylation in pressure overload-induced hypertrophied mouse hearts through a receptor-mediated mechanism. *Am J Physiol Cell Physiol*. 2010;**299**(6):C1524-9.
39. Cao X, Kambe F, Moeller LC, et al. Thyroid hormone induces rapid activation of Akt/protein kinase B-mammalian target of rapamycin-p70S6K cascade through phosphatidylinositol 3-kinase in human fibroblasts. *Mol Endocrinol*. 2005;**19**(1):102-12.
40. Alonso-Merino E, Martin Orozco R, Ruiz-Llorente L, et al. Thyroid hormones inhibit TGF-beta signaling and attenuate fibrotic responses. *Proc Natl Acad Sci U S A*. 2016;**113**(24):E3451-60.
41. Brown AR, Simmen RC, Simmen FA. The role of thyroid hormone signaling in the prevention of digestive system cancers. *Int J Mol Sci*. 2013;**14**(8):16240-57.
42. Li M, Iismaa SE, Naqvi N, et al. Thyroid hormone action in postnatal heart development. *Stem Cell Res*. 2014;**13**(3 Pt B):582-91.
43. Francavilla A, Carr BI, Azzarone A, et al. Hepatocyte proliferation and gene expression induced by triiodothyronine in vivo and in vitro. *Hepatology*. 1994;**20**(5):1237-41.
44. Bockhorn M, Frilling A, Benko T, et al. Tri-iodothyronine as a stimulator of liver regeneration after partial and subtotal hepatectomy. *Eur Surg Res*. 2007;**39**(1):58-63.
45. Fanti M, Singh S, Ledda-Columbano GM, et al. Tri-iodothyronine induces hepatocyte proliferation by protein kinase A-dependent beta-catenin activation in rodents. *Hepatology*. 2014;**59**(6):2309-20.
46. Dentice M, Ambrosio R, Damiano V, et al. Intracellular inactivation of thyroid hormone is a survival mechanism for muscle stem cell proliferation and lineage progression. *Cell Metab*. 2014;**20**(6):1038-48.
47. Franco PG, Silvestroff L, Soto EF, et al. Thyroid hormones promote differentiation of oligodendrocyte progenitor cells and improve remyelination after cuprizone-induced demyelination. *Exp Neurol*. 2008;**212**(2):458-67.
48. Eaves CJ. Cancer stem cells: Here, there, everywhere? *Nature*. 2008;**456**(7222):581-2.
49. Ciavardelli D, Bellomo M, Crescimanno C, et al. Type 3 deiodinase: role in cancer growth, stemness, and metabolism. *Front Endocrinol (Lausanne)*. 2014;**5**:215.

50. Chatonnet F, Guyot R, Benoit G, et al. Genome-wide analysis of thyroid hormone receptors shared and specific functions in neural cells. *Proc Natl Acad Sci U S A*. 2013;**110**(8):E766-75.
51. Ramadoss P, Abraham BJ, Tsai L, et al. Novel mechanism of positive versus negative regulation by thyroid hormone receptor beta1 (TRbeta1) identified by genome-wide profiling of binding sites in mouse liver. *J Biol Chem*. 2014;**289**(3):1313-28.
52. Bernal J, Guadano-Ferraz A, Morte B. Thyroid hormone transporters-functions and clinical implications. *Nat Rev Endocrinol*. 2015;**11**(12):690.
53. Visser TJ. Cellular Uptake of Thyroid Hormones. In: De Groot LJ, Chrousos G, Dungan K, Feingold KR, Grossman A, Hershman JM, et al., editors. Endotext. South Dartmouth (MA)2000.
54. Rooman I, Lutz C, Pinho AV, et al. Amino acid transporters expression in acinar cells is changed during acute pancreatitis. *Pancreatology*. 2013;**13**(5):475-85.

*55. Sohal, D.S., M. Nghiem, M.A. Crackower, S.A. Witt, T.R. Kimball, K.M. Tymitz, J.M. Penninger, and J.D. Molkentin, *Temporally regulated and tissue-specific gene manipulations in the adult and embryonic heart using a tamoxifen-inducible Cre protein.* Circ Res, 2001. **89**(1): p. 20-5.

*56. Bombardo, M., E. Malagola, R. Chen, A. Rudnicka, R. Graf, and S. Sonda, *Ibuprofen and diclofenac treatments reduce proliferation of pancreatic acinar cells upon inflammatory injury and mitogenic stimulation.* Br J Pharmacol, 2017.

*57. Graf, R., M. Schiesser, A. Lussi, P. Went, G.A. Scheele, and D. Bimmler, *Coordinate regulation of secretory stress proteins (PSP/reg, PAP I, PAP II, and PAP III) in the rat exocrine pancreas during experimental acute pancreatitis.* J Surg Res, 2002. **105**(2): p. 136-44.

*Cited only in supplementary materials.

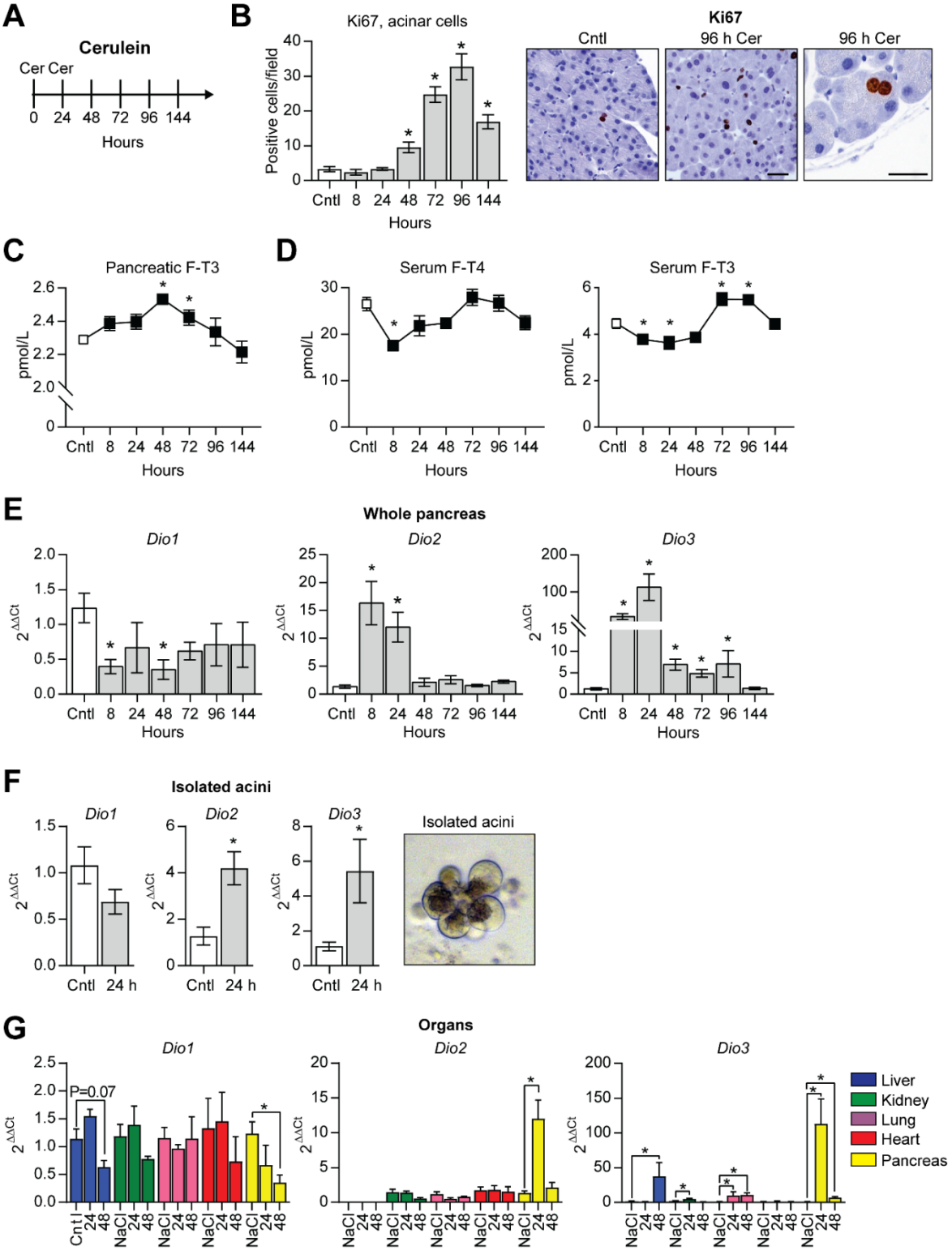
A
Cerulein
Cer Cer
0 24 48 72 96 144
Hours
B
Ki67, acinar cells
Positive cells/field
Cntl 8 24 48 72 96 144
Hours
Ki67
Cntl
96 h Cer
96 h Cer
C
Pancreatic F-T3
pmol/L
Cntl 8 24 48 72 96 144
Hours
D
Serum F-T4
pmol/L
Cntl 8 24 48 72 96 144
Hours
Serum F-T3
pmol/L
Cntl 8 24 48 72 96 144
Hours
E
Whole pancreas
Dio1
Dio2
Dio3
2^-ΔΔCt
Cntl 8 24 48 72 96 144
Hours
F
Isolated acini
Dio1
Dio2
Dio3
2^-ΔΔCt
Cntl 24 h
Isolated acini
G
Organs
Dio1
Dio2
Dio3
2^-ΔΔCt
P=0.07
Cntl 24 48 NaCl 24 48
Liver
Kidney
Lung
Heart
Pancreas

Figure 1

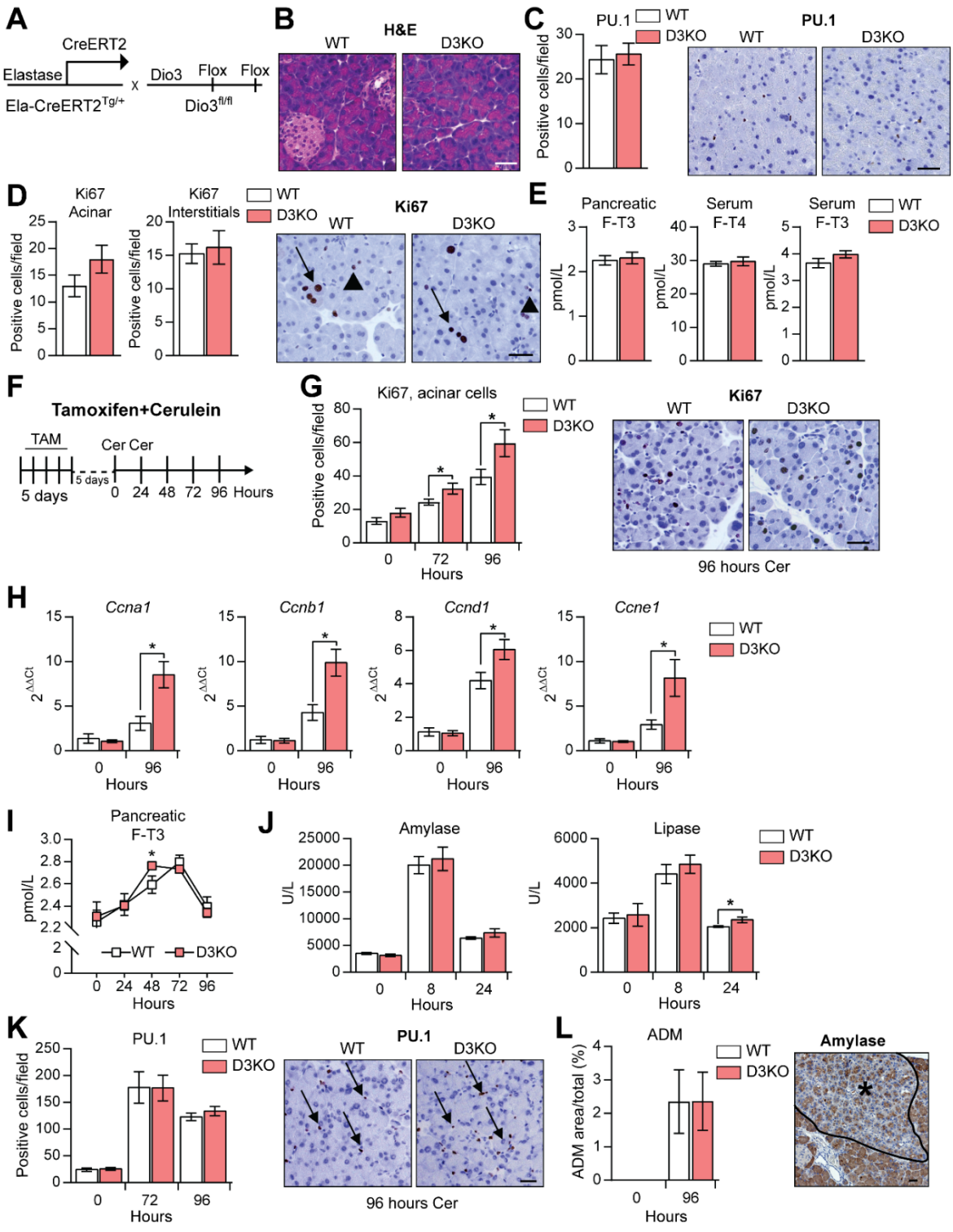
A
CreERT2
Elastase
Ela-CreERT2Tg/+
x
Dio3 Flox Flox
Dio3fl/fl
B
H&E
WT
D3KO
C
PU.1
WT
D3KO
Positive cells/field
PU.1
WT
D3KO
D
Ki67 Acinar
Ki67 Interstitials
WT
D3KO
Positive cells/field
Ki67
WT
D3KO
E
Pancreatic F-T3
Serum F-T4
Serum F-T3
pmol/L
WT
D3KO
F
Tamoxifen+Cerulein
TAM
5 days
Cer Cer
5 days
0 24 48 72 96 Hours
G
Ki67, acinar cells
Positive cells/field
WT
D3KO
Hours
Ki67
WT
D3KO
96 hours Cer
H
Ccna1
Ccnb1
Ccnd1
Ccne1
2-ΔΔCt
WT
D3KO
Hours
I
Pancreatic F-T3
pmol/L
WT
D3KO
Hours
J
Amylase
Lipase
U/L
WT
D3KO
Hours
K
PU.1
WT
D3KO
Positive cells/field
Hours
PU.1
WT
D3KO
96 hours Cer
L
ADM
WT
D3KO
ADM area/total (%)
Hours
Amylase

Figure 2

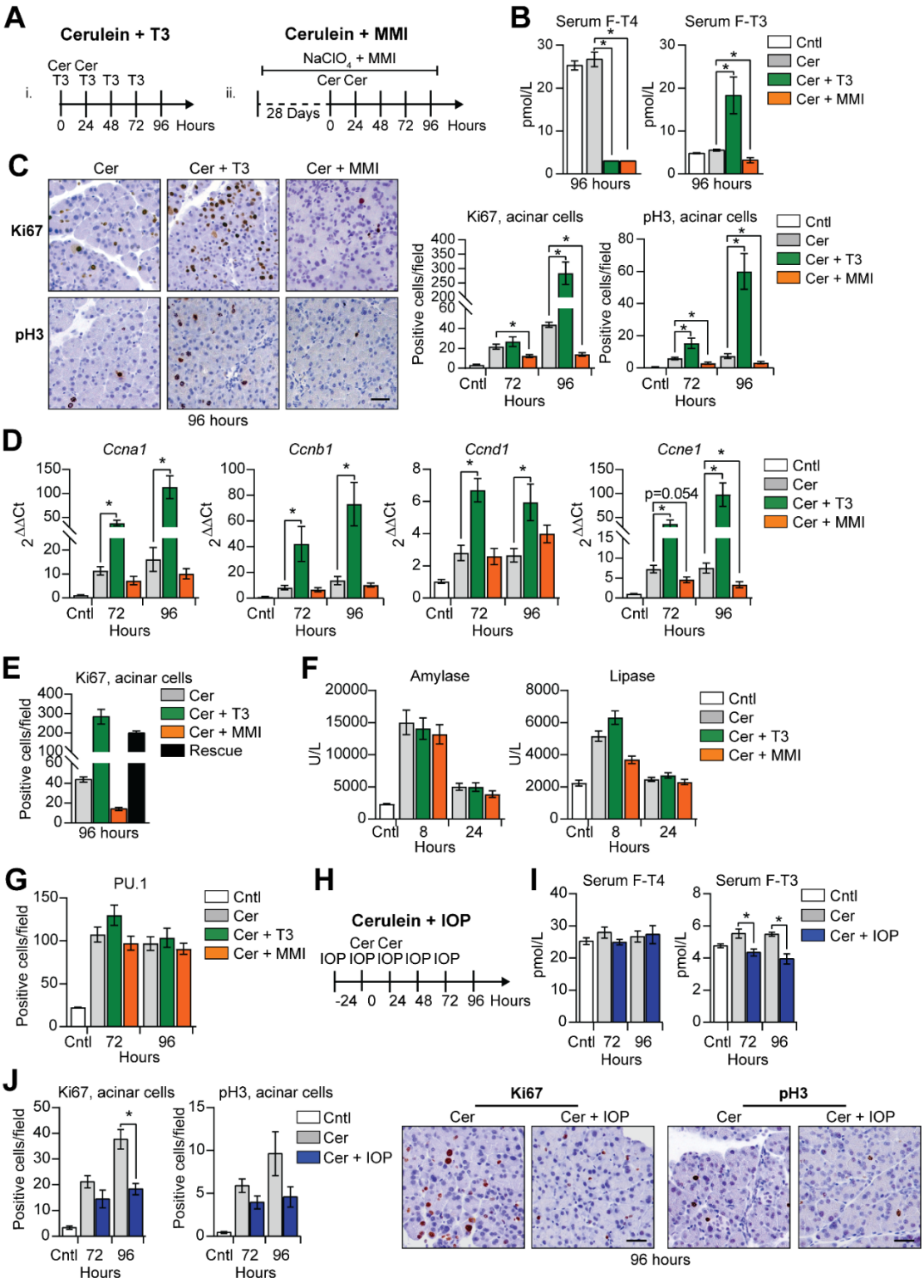
A
Cerulein + T3
Cer Cer
T3 T3 T3 T3
i.
0 24 48 72 96 Hours
Cerulein + MMI
NaClO4 + MMI
Cer Cer
ii.
28 Days
0 24 48 72 96 Hours
B
Serum F-T4
Serum F-T3
pmol/L
96 hours
Cntl
Cer
Cer + T3
Cer + MMI
C
Cer
Cer + T3
Cer + MMI
Ki67
pH3
96 hours
Ki67, acinar cells
pH3, acinar cells
Positive cells/field
Cntl 72 96
Hours
D
Ccna1
Ccnb1
Ccnd1
Ccne1
2ΔΔCt
p=0.054
E
Ki67, acinar cells
Rescue
F
Amylase
Lipase
U/L
G
PU.1
H
Cerulein + IOP
Cer Cer
IOP IOP IOP IOP IOP
-24 0 24 48 72 96 Hours
I
Cer + IOP
J
Ki67
pH3

Figure 3

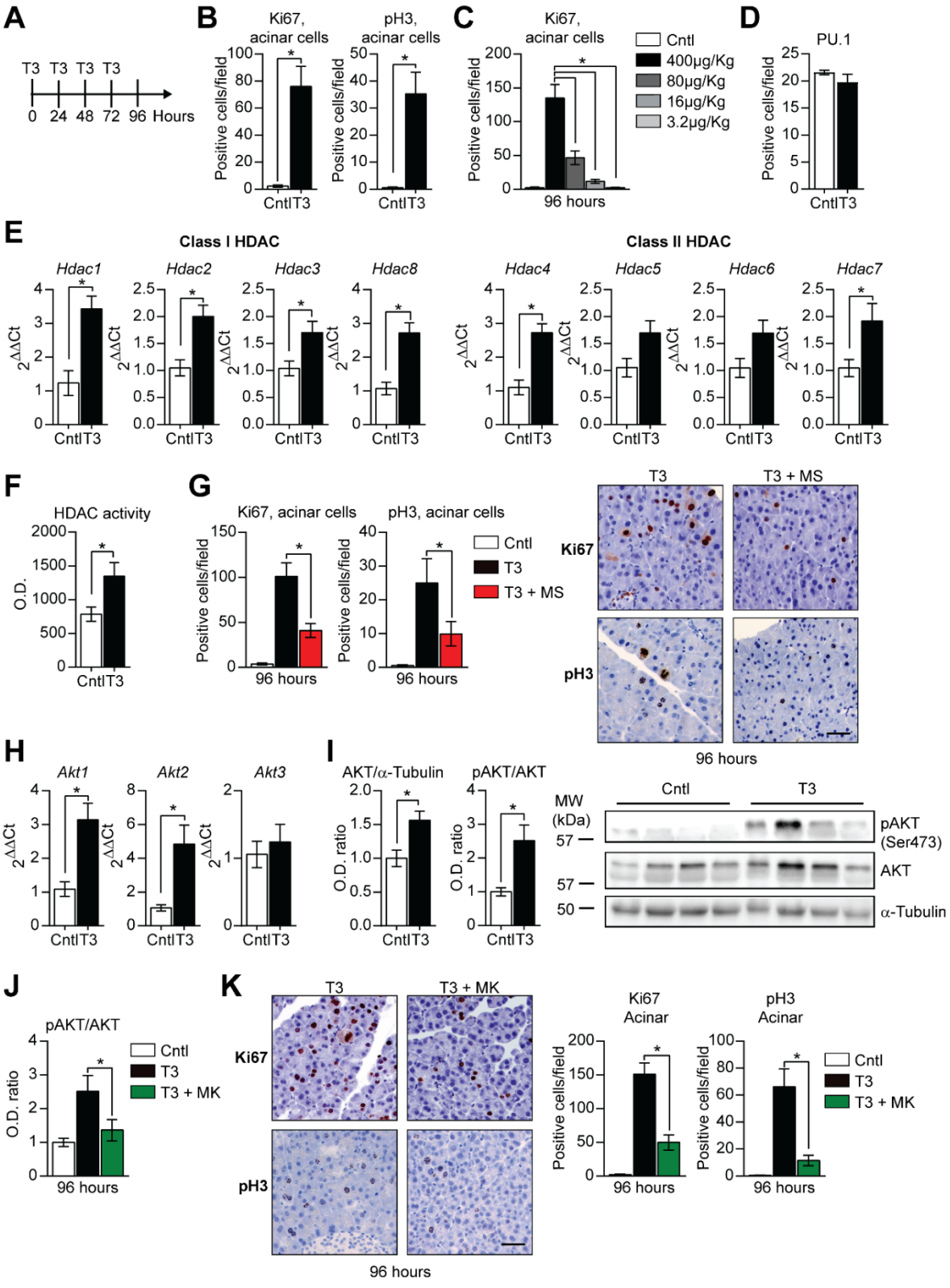
A
T3 T3 T3 T3
0 24 48 72 96 Hours
B
Ki67, acinar cells
pH3, acinar cells
Positive cells/field
Cntl T3
C
Ki67, acinar cells
Cntl
400µg/Kg
80µg/Kg
16µg/Kg
3.2µg/Kg
96 hours
D
PU.1
E
Class I HDAC
Class II HDAC
Hdac1
Hdac2
Hdac3
Hdac8
Hdac4
Hdac5
Hdac6
Hdac7
2ΔΔCt
F
HDAC activity
O.D.
G
Ki67, acinar cells
pH3, acinar cells
Cntl
T3
T3 + MS
96 hours
T3
T3 + MS
Ki67
pH3
H
Akt1
Akt2
Akt3
I
AKT/α-Tubulin
pAKT/AKT
O.D. ratio
MW (kDa)
pAKT (Ser473)
AKT
α-Tubulin
J
pAKT/AKT
T3 + MK
K
T3
T3 + MK
Ki67 Acinar
pH3 Acinar

Figure 4

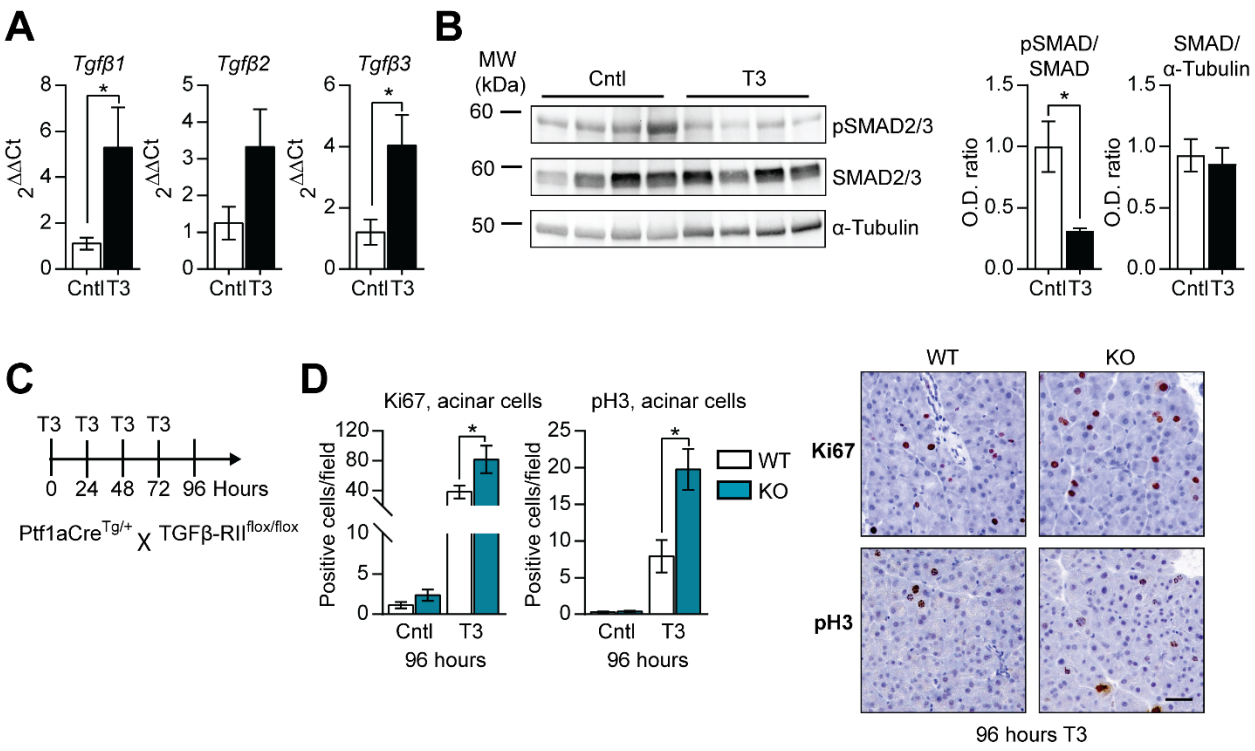
A
Tgfβ1
Tgfβ2
Tgfβ3
2ΔΔCt
Cntl T3
B
MW (kDa)
Cntl
T3
60
60
50
pSMAD2/3
SMAD2/3
α-Tubulin
pSMAD/ SMAD
SMAD/ α-Tubulin
O.D. ratio
C
T3 T3 T3 T3
0 24 48 72 96 Hours
Ptf1aCre^Tg/+ X TGFβ-RII^flox/flox
D
Ki67, acinar cells
pH3, acinar cells
Positive cells/field
96 hours
WT
KO
Ki67
pH3
96 hours T3

Figure 5

SUPPLEMENTARY INFORMATION

MATERIALS AND METHODS

Animal experiments

Mice used in this study were C57BL/6 mice (Envigo, Itingen, Switzerland), TGF-RII KO mice bred in our facility by crossing mice expressing TGFβ receptor II$^{flox/flox}$ $_{with}$ mice harbouring pancreas transcription factor 1a (PTF1a) promoter Cre transgene (PTF1acre; MMRRC, USA), and D3KO mice bred in our facility. D3KO animals were generated by crossing mice harboring elastase (ELA) promoter driven Cre transgene ELA$^{CreERT2Tg/+}$ [19] with transgenic mice expressing Deiodinase 3 $^{flox/flox}$ [45].

Tamoxifen (Sigma-Aldrich, Buchs, Switzerland)-driven recombination was induced with 100 µL injection of 20 mg/mL tamoxifen daily for five consecutive days as described [55].

Acute pancreatitis was induced via six intraperitoneal (i.p.) injections of 50 µg/kg cerulein (Sigma-Aldrich, Buchs, Switzerland), administered hourly on two consecutive days. Control animals received 0.9% NaCl injections. Hyperthyroidism was induced with daily injections of 400 µg/kg T3 (Sigma-Aldrich, Buchs, Switzerland). Control animals received vehicle 0.1 M NaOH, pH 7.4 with 0.5% BSA injections. Hypothyroidism was induced by administration of 1% $NaClO_4$ and 0.1% methimazole (MMI, Sigma-Aldrich, Buchs, Switzerland) in drinking water for 28 days [10].

Class I histone deacetylase (HDAC) inhibitor MS-275 (Selleckchem, Houston, USA) was injected daily i.p. at 20 mg/kg, starting one day before the first T3 injection (See scheme Fig.S4).

Akt inhibitor MK-2206 (A3010, APExBIO, Houston, USA) was injected four times daily i.p. at 8 mg/kg, starting before the first T3 injection (see scheme Fig.S5).

Immunohistochemistry

Primary antibodies used in this study were: rabbit anti-Ki67 (#ab16667, Abcam, Cambridge, UK, 1:200); rabbit anti-phospho-H3(06-570, Millipore); rabbit anti-amylase (#A8273-1VL, Sigma-Aldrich, Buchs, Switzerland, 1:1000); rabbit anti-PU.1 (#2266, Cell Signaling Technologies, Danvers, MA, 1:200); rabbit anti-phospho-histone H2A.X (Ser139) (#9718, Cell Signaling Technologies, Danvers, MA, 1:500); rabbit anti-cleaved Caspase-3 (Asp175) (#9661, Cell Signaling Technologies, Danvers, MA, 1:1500). Secondary antibodies used in this study were biotinylated goat anti-rabbit IgG (H + L), included in the Vectastain® ABC Kit (PK-4001, Vector Laboratories, Peterborough, UK). All staining, with the exception of amylase, was performed with a DAKO autostainer Link 48 (Glostrup, Denmark).

Microscopy analyses were performed on a wide-field Nikon Eclipse Ti (Amsterdam, The Netherlands). Quantification of labelled cells was performed in at least ten randomly selected high-power fields (×200) per slide using the NIS Elements BR Analysis (Nikon, Amsterdam, The Netherlands) and Cell^P (Olympus, Tokyo, Japan) analysis software. Number of positive cells was normalized based upon the area exclusively occupied by pancreatic acinar tissue present in each power field. Area occupied by pancreatic ducts, islets and vessels were excluded from the analysis.

Quantitative analysis of acinar-to-ductal metaplasia (ADM) was performed as described in an earlier paper from our group [56]. Briefly, paraffin-embedded pancreas specimens were immunostained for amylase, slides were scanned with a NDP NanoZoomer Digital Pathology Slide Scanner (Hamamatsu, Solothurn, Switzerland) and analyzed for ADM lesions in a blinded fashion. ADM present in the entire pancreas slide of individual mice were quantified by manual counting. ADM were identified according to: i) loss of amylase content, ii) structural re-organization into tubular

complexes, iii) stromal reaction characterized by presence of cell infiltrates. The area occupied by ADM was expressed as a percentage of total pancreatic area present in each slide.

Western blotting

Twenty mg of pancreatic tissue was homogenized in RIPA buffer containing a protease inhibitor cocktail (Roche Diagnostics, Rotkreuz, Switzerland). Protein concentrations were determined by a Bradford protein assay (BioRad, Hercules, CA). 20 μg of proteins were resolved by SDS-PAGE electrophoresis and blotted onto nitrocellulose membranes using a V3 Western Workflow system (BioRAd, Hercules, CA) according to the manufacturer's protocols. Membranes were incubated with primary antibodies overnight at 4°C. Primary antibodies used in this study were: phospho-AKT (4051, Cell Signaling, Danvers, MA); AKT (9272, Cell Signaling, Danvers, MA); α-tubulin (2125, Cell Signaling, Danvers, MA); phospho-SMAD2/3 (Ser423/425) (8828, Cell Signaling, Danvers, MA); SMAD2/3 (8685, Cell Signaling, Danvers, MA).

Transcript analyses

Total RNA was extracted from pancreatic tissue, as described previously [57], and RNA quality control was performed by RIN (RNA Integrity Number) measurement using a 2100 Bioanalyzer system (Agilent, Santa Clara, CA). RNA was reverse-transcribed with qScript™ cDNA SuperMix (Quanta Biosciences, Beverly, MA). Gene expression was measured by real-time PCR on a 7500 Fast Real-Time PCR System (Applied Biosystems, Foster City, CA).

Biochemical analyses

Levels of enzymatic activity of amylase, lipase and LDH were measured in blood serum collected via heart puncture. Enzyme activities were measured using the Fuji Dri-Chem 4000i analyzer (FUJIFILM Corporation, Tokyo, Japan).

Blood levels of F-T4 and F-T3 were quantified with Cobas 8000 Modular-System e602 analyzer (Roche Diagnostics, Rotkreuz, Switzerland), according to the manufacturer's instructions.

Tissue levels of F-T3 were measured using an Elisa Kit (CUSABIO Technology LLC, Houston, TX) according to the manufacturer instruction.

Nuclear protein extraction and HDAC activity

Nuclear proteins were extracted from 20 mg of pancreatic tissue with the EpiQuik™ Nuclear Extraction Kit (Epigentek Group Inc., Mountain View, CA) and HDAC activity was measured in the nuclear extracts with the fluorimetric EpiQuik HDAC Activity/Inhibition Assay Kit (Epigentek Group Inc. Mountain View, CA), following the manufacturer's instructions.

SUPPLEMENTARY FIGURE LEGENDS

Figure S1. (A) Representative microphotographs of Ki67 stained cells (complete field of view). **(B)** Quantification of amylase and lipase activity in serum in untreated mice. **(C)** Quantification of Ki67 and pH3-positive acinar cells in untreated mice, one month after tamoxifen treatment. Right panels, representative microphotographs of stained cells. Results are average ± SEM (n=5), *P < 0.05. Scale bars: 50 μm.

Figure S2. (A) Quantification of Ki67-positive acinar cells, expressed as percentage of total acinar cell number, 96 hours after induction of pancreatitis upon hyperthyroidism and hypothyroidism with T3 and MMI administration, respectively. **(B)**

Quantification of acinar cell size 96 hours after induction of pancreatitis. Results are average ± SEM (n=5), *P < 0.05.

Figure S3. Quantification of lactate dehydrogenase (LDH) activity in serum 8 hours after induction of pancreatitis. Results are average ± SEM (n=5), *P < 0.05.

Figure S4. (A) Quantification of acinar cells positive for the apoptotic marker cleaved caspase 3, 96 hours after induction of pancreatitis. Right panel, representative microphotographs of stained cell. **(B)** Quantification of acinar cells positive for the DNA damage marker pH2AX 96 hours after induction of pancreatitis. Right panels, representative microphotograph of stained cell. Results are average ± SEM (n=5), *P < 0.05. Scale bars: 50 μm.

Figure S5. (A) qPCR of cyclin expression in the pancreas 96 hours after T3 administration. Cyclin A (*Ccna1*), cyclin B (*Ccnb1*), cyclin D (*Ccnd1*), cyclin E (*Ccne1*). **(B)** Hematoxylin and Eosin (H&E) staining of pancreata 96 hours after T3 administration. Results are average ± SEM (n=5), *P < 0.05. Scale bars: 50 μm.

Figure S6. (A) Representative microphotograph of Ki67 stained cells in the heart 96 hours after T3 administration. **(B)** Quantification of Ki67-positive islet cells at the indicated time of T3 administration. Right panel, representative microphotograph of Ki67 stained cells in the pancreas 96 hours after T3 administration.Arrow, islet of Langherans. Results are average ± SEM (n=5), *P < 0.05. Scale bars: 50 μm.

Figure S7. (A) Schematic representation of T3 treatment in the presence of the selective class I inhibitor MS-275 (MS). **(B)** Quantification of HDAC activity in the pancreas 96 hours after T3 treatment in the presence of MS. **(C)** qPCR of cyclin expression in the pancreas 96 hours after T3 treatment in the presence of MS. Cyclin A (*Ccna1*), cyclin B (*Ccnb1*), cyclin D (*Ccnd1*), cyclin E (*Ccne1*). **(D)** qPCR of cell cycle

inhibitor expression in the pancreas 96 hours after T3 treatment in the presence of MS. Results are average ± SEM (n=5), *P < 0.05.

Figure S8. (A) Schematic representation of T3 treatment in the presence of the selective AKT inhibitor MK-2206 (MK). **(B)** qPCR of cyclin expression in the pancreas 96 hours after T3 treatment in the presence of MK. Cyclin A (*Ccna1*), cyclin B (*Ccnb1*), cyclin D (*Ccnd1*), cyclin E (*Ccne1*). **(C)** qPCR of cell cycle inhibitor expression in the pancreas 96 hours after T3 treatment in the presence of MK. P15 (*Cdkn2b*), p16 (*Cdkn2a*), p18 (*Cdkn2c*), p21 (*Cdkn1a*), p27 (*Cdkn1b*). Results are average ± SEM (n=5), *P < 0.05.

Figure S9. (A) qPCR of cyclin expression in the pancreas 96 hours after T3 treatment in wild type (WT) and TGFβ receptor II deficient (KO) mice. **(C)** qPCR of cell cycle inhibitor expression in the pancreas 96 hours after T3 treatment. P15 (*Cdkn2b*), p16 (*Cdkn2a*), p18 (*Cdkn2c*), p21 (*Cdkn1a*), p27 (*Cdkn1b*). Results are average ± SEM (n=5), *P < 0.05.

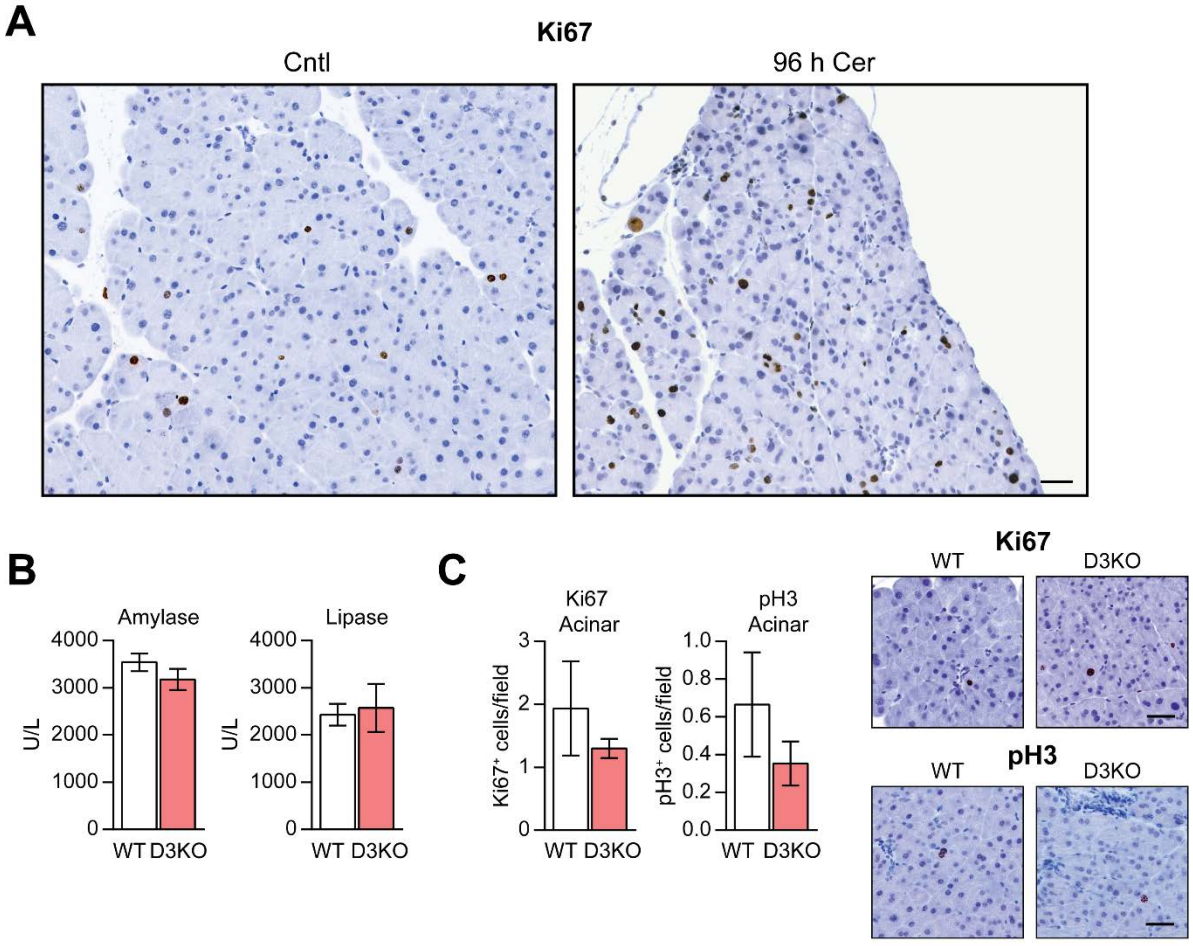

Figure S1

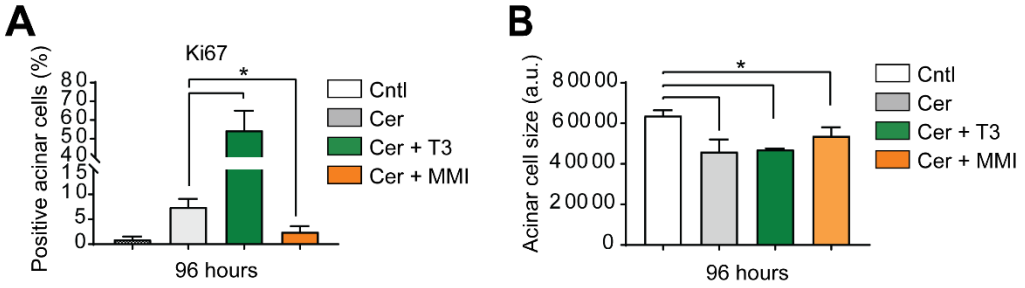

Figure S2

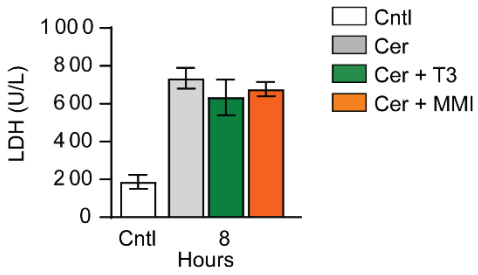

Figure S3

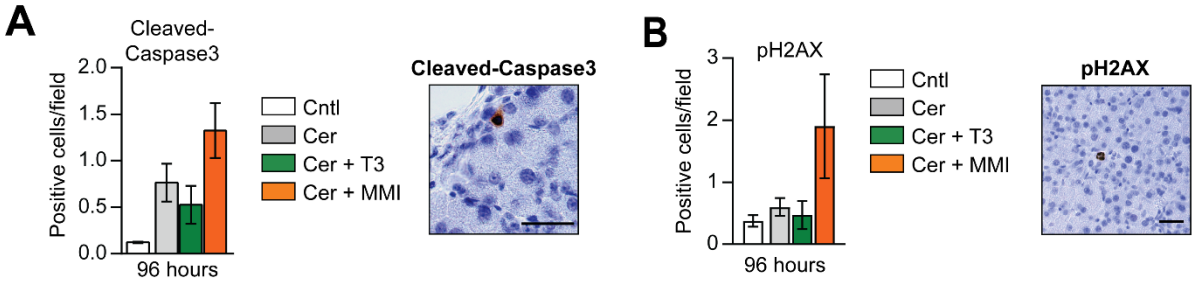

Figure S4

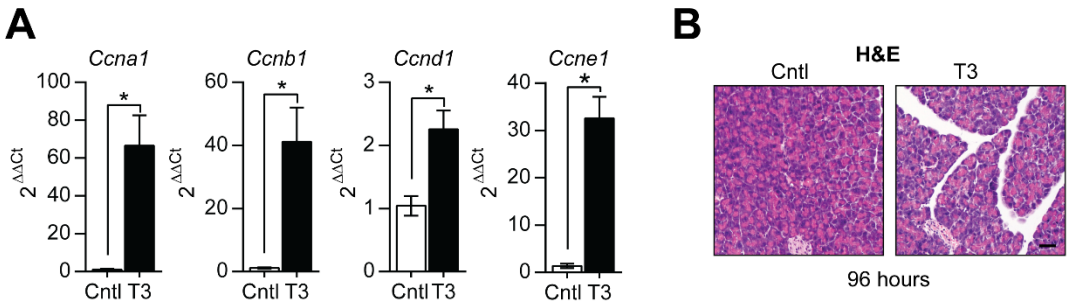

Figure S5

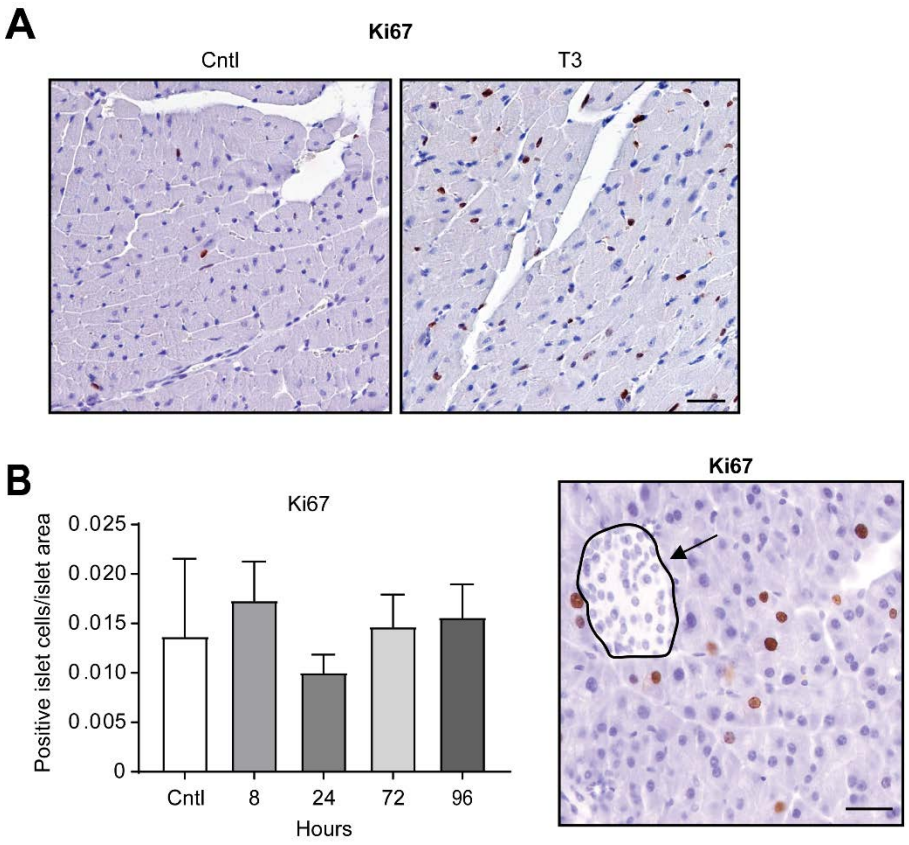

Figure S6

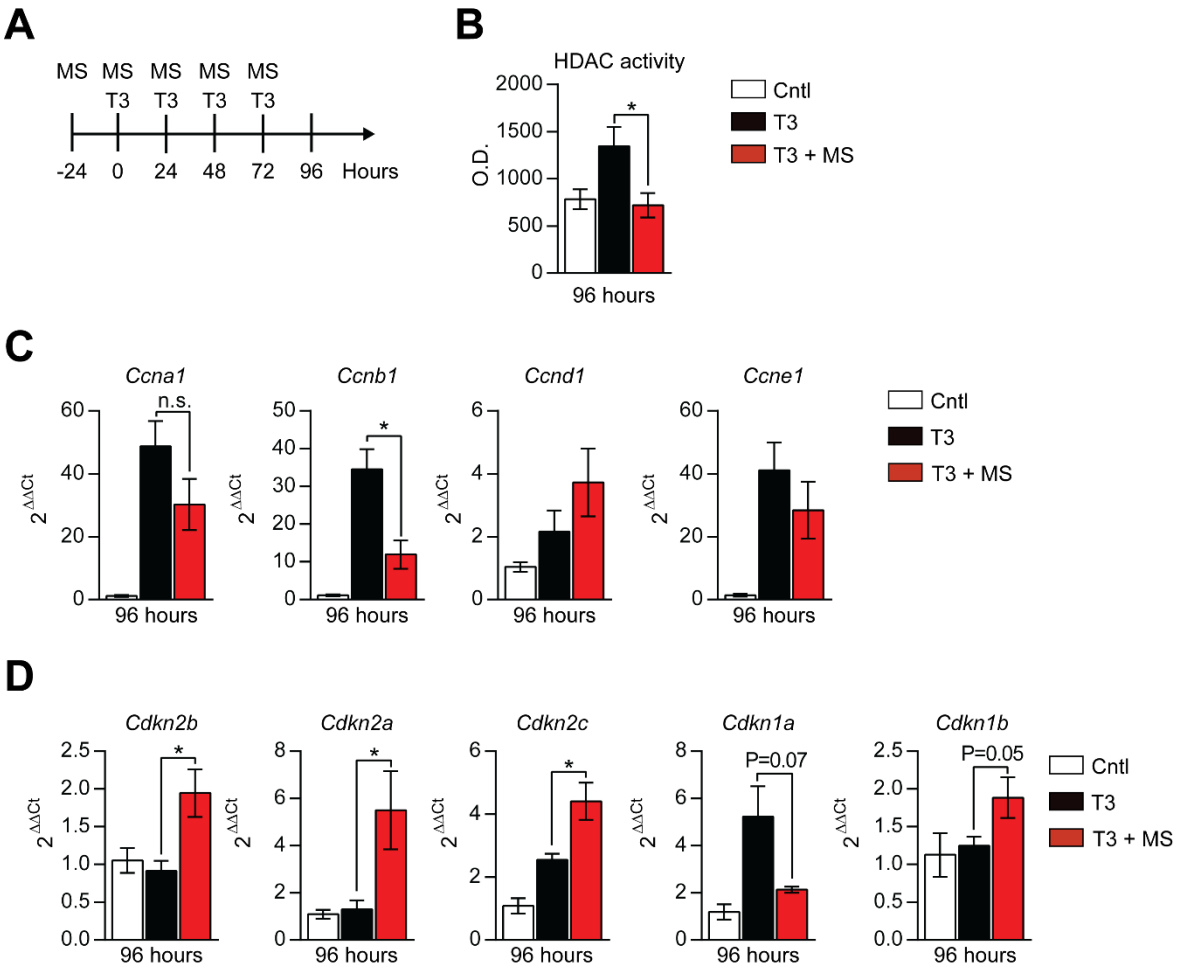
A
MS MS MS MS MS
T3 T3 T3 T3
-24 0 24 48 72 96 Hours
B
HDAC activity
O.D.
2000
1500
1000
500
0
*
96 hours
Cntl
T3
T3 + MS
C
Ccna1
n.s.
Ccnb1
*
Ccnd1
Ccne1
2^ΔΔCt
60
40
20
0
50
30
10
6
4
2
96 hours
Cntl
T3
T3 + MS
D
Cdkn2b
Cdkn2a
Cdkn2c
Cdkn1a
P=0.07
Cdkn1b
P=0.05
2.5
2.0
1.5
1.0
0.5
0.0
8
96 hours
Cntl
T3
T3 + MS

Figure S7

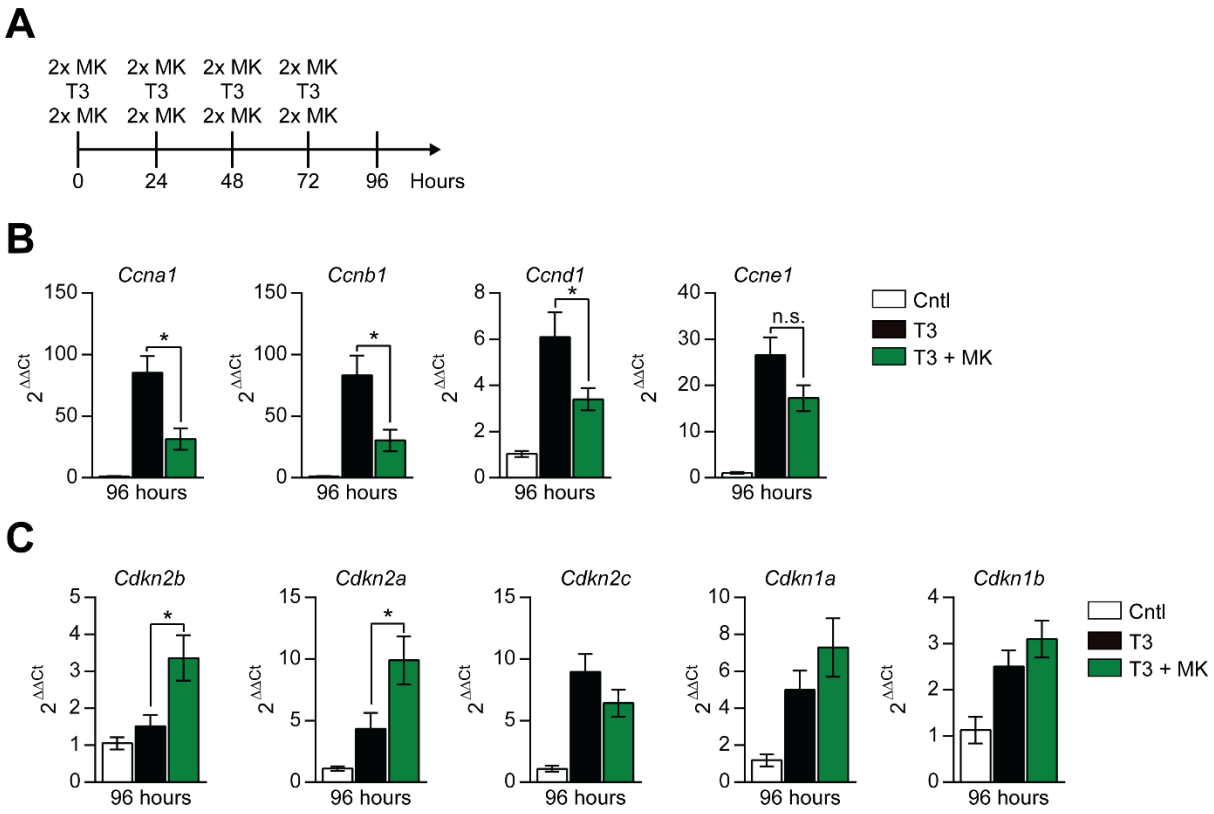

Figure S8

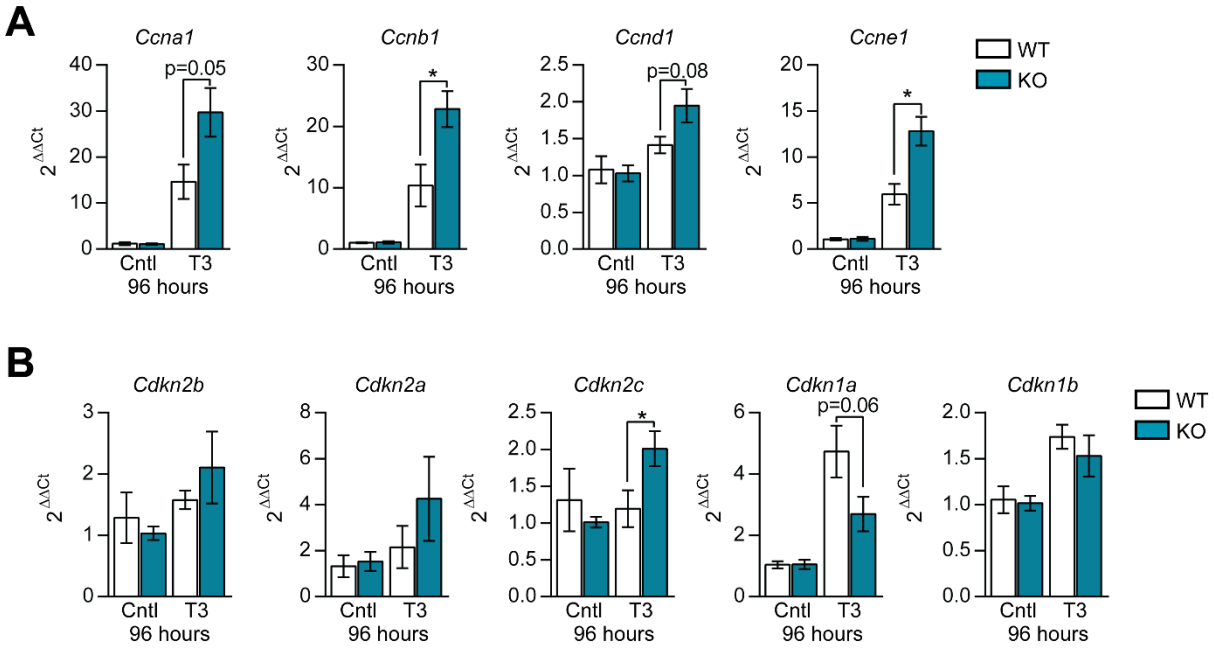

Figure S9